Rheological and Structural Characterization of Hydrophobically Modified Polyacrylamide Solutions in the Semidilute Regime

Valeria Castelletto,*,† Ian W. Hamley,† Wei Xue,† Cornelia Sommer,‡ Jan Skov Pedersen,‡ and Peter D. Olmsted§

Department of Chemistry, University of Leeds, Leeds LS2 9JT, U.K., Department of Chemistry, University of Aarhus, Langelandsgade 140, DK-8000 Aarhus C, Denmark, and Department of Physics and Astronomy, University of Leeds, Leeds LS2 9JT, U.K.

Received July 20, 2003

ABSTRACT: Semidilute solutions of two series of polyacrylamide (AM)-based copolymers containing hydrophobic di-*n*-propylacrylamide (DPAM) and di-*n*-octylacrylamide (DOAM) comonomers, namely P(DPAM-*co*-AM) and P(DOAM-*co*-AM), have been characterized using rheology and small angle X-ray scattering (SAXS). The relaxation time and plateau modulus obtained from rheology, and the correlation length (ξ) obtained from SAXS are compared for copolymers with different hydrophobe content (f) and hydrophobe block length (N_H). Shear rheometry experiments revealed that P(DOAM-*co*-AM) copolymers formed gels characterized by a broad distribution of relaxation modes. In contrast, solutions of P(DPAM-*co*-AM) copolymers exhibited a near-Maxwellian response although additional fast modes contribute significantly to the dynamic shear modulus at high frequency. For both copolymers, the dynamic shear moduli obtained at different temperatures could be time−temperature superposed, with a shift factor described by the Williams−Landel−Ferry equation. For P(DPAM-*co*-AM) solutions, the sticker lifetime (determined from the fitting of the dynamic moduli to a Maxwell model) was found to increase with increasing f but to be insensitive to N_H, in the range examined. However, the plateau modulus G_o decreases with increasing N_H, which is related to the increase in strand length between stickers. Similar to P(DPAM-*co*-AM) solutions, one relaxation time for the gels of copolymers with longer hydrophobes (in this case determined from the crossover in the elastic moduli) is more sensitive to f than to N_H. The SAXS data for the P(DPAM-*co*-AM) solutions could be modeled using the structure factor for a polymer solution in a good solvent although enhanced fluctuations had to be considered for the polymers with higher hydrophobe content. The correlation length was found to decrease with increasing temperature for P(DPAM-*co*-AM) solutions, due an improvement of the solvent quality. But ξ did not depend on the temperature for P(DOAM-*co*-AM) samples, probably due to stronger associations between hydrophobes. Trends of ξ with N_H and f are discussed.

1. Introduction

Polymers that act as associative thickeners in water are of considerable industrial importance in paint coatings, personal care products, and oil industries because of their ability to dramatically modify rheological properties. They consist of chains of predominantly hydrophilic repeat units but also incorporate a small fraction of hydrophobic sequences in the main chain or as side groups. Even with only 1−2% of a hydrophobe, a dramatic increase in viscosity can be achieved. This results from intra- and intermolecular associations of the hydrophobic groups, forming effectively a physically cross-linked gel structure.

A number of classes of associating polymer have now been developed.[1−5] A particularly important class are telechelic end-capped copolymers such as the HEUR (hydrophobic ethyoxylated urethane) associative thickeners, which comprise poly(ethylene glycol), chain extended by diisocyanates, and end-capped by long-chain alcohols.[6−9] Analogous F−HEUR polymers,[10−17] are terminated at both ends with hydrophobic fluoroalkyl segments. These are much more effective thickeners compared to the corresponding hydrocarbon derivatives.[11−13]

Another widely investigated type are the HASE (hydrophobically modified alkali-swellable) thickeners, which are copolymers of ethyl acrylate and methacrylic acid, containing a small fraction of hydrophobic substituents.[2] In contrast to the telechelic end-capped copolymers such as HEUR and F−HEUR, HASE polymers have a comblike architecture, with *n*-alkyl hydrophobes tethered to the backbone via polyether side chains.[18,19]

Copolymers based on polyacrylamide and its derivatives, especially hydrophobically modified polyacrylamide (HM−PAM)[20−22] and hydrophobically modified poly(*N*-isopropylacrylamide) (HM−PNIPAM)[23,24] have attracted great interest as hydrophobically associating polymers. Similarly to HASE polymers, these are multisticker copolymers, in which the pendant hydrophobic groups are randomly distributed along the chain. In contrast to telechelic polymers, the number of hydrophobic units is greater than two and the "stickers" are distributed randomly in the polymer backbone leading to profound differences in the network structure dynamics between the two systems, allowing for example the possibility of so-called superbridges.[7] HM−PAM polymers are relatively polydisperse and generally have higher molecular weight than telechelic polymers and therefore the chain motion in concentrated solution is influenced by reptation as a consequence of entanglements.

* Author for correspondence.
† Department of Chemistry, University of Leeds.
‡ Department of Chemistry, University of Aarhus.
§ Department of Physics and Astronomy, University of Leeds.

10.1021/ma035039d CCC: $27.50
Published on Web 01/24/2004

The rheology of HM−PAM associative polymers containing alkylacrylamide hydrophobic comonomers has been studied in detail.[25,26] The shear rate dependence of the viscosity, and the concentration dependence of the viscosity in solutions below the overlap concentration have been measured.[25] The scaling of viscosity with concentration, hydrophobe content and hydrophobe block length has been compared[26] to the predictions of the model of Leibler et al. for the rheology of multisticker chains.[27] The viscoelastic behavior of semidilute solutions of various series of copolymers with variable molecular weight, hydrophobe content, and hydrophobe block length has been investigated as a function of the polymer concentration. The linear viscoelasticity could be described by a slow relaxation process with a plateau modulus that only depends on polymer concentration; in addition, several fast relaxation processes were observed.[26]The relaxation process was also studied in a series of perfluoroalkyl end-capped poly(oxyethylene) (PEO) F−HEUR associative copolymers.[14,16] The stress relaxation was measured as a function of the polymer concentration. It was found that it could be fitted in all cases using a stretched exponential, which is widely used to model relaxation processes in complex, slowly relaxing, strongly interacting materials.[28]

The dynamics of networks formed by telechelic associative thickeners[29] are predicted to be dominated by the detachment of hydrophobic end groups from the clusters, such that the motion of the chain is governed by a detachment time plus the Rouse motion of the detached chain.[29] For HEUR associative polymers, a relaxation time related to the network relaxation has been noted, in addition to the relaxation time corresponding to the lifetime of the hydrophobe in the micellar junction.[30]

The relationship between structure and rheology for associative triblock copolymers fully end capped with alkyl chains has recently been interpreted in terms of the structure and interactions of flowerlike micelles.[31] The micelles were treated as adhesive hard spheres. It was found that at low concentrations the rheology is dominated by pairwise interactions between associating spherical micelles. However, as the concentration increases, the density of bridging chains increases and the behavior approaches the ideal transient network limit.

Besides rheology, small angle scattering (SAS) has been widely used to study the structure of associative polymer gels.[17,32] Surprisingly, although SAS has already been used to study PAM and PNIPAM gels,[33,34] we are not aware of any SAS studies on solutions of HM−PAM or HM−PNIPAM.

From a theoretical viewpoint, the association properties (size and shape of hydrophobic aggregates) and linear rheology of polymers with end stickers have been modeled.[27,35−42] Computer simulations of reversibly associating polymers with sticker groups along the backbone have also been performed.[43,44] Recent work has suggested that close to the critical temperature for polymer−solvent phase separation in an associating polymer solution, the sol−gel transition has a thermodynamic signature reminiscent of the micellization of surfactant solutions. However, at high temperatures, gelation was found to be a continuous transition.[44]

In this work, we study the rheology and structure of aqueous solutions of hydrophobically modified polyacrylamide (AM: acrylamide) copolymers in semidilute solution. The disubstituted acrylamides di-*n*-propylacrylamide (DPAM) and di-*n*-octylacrylamide (DOAM) have been used as hydrophobic comonomers to produce poly(di-*n*-propylacrylamide-*co*-acrylamide) (P(DPAM-*co*-AM)) and poly(di-*n*-octylacrylamide-*co*-acrylamide) (P(DOAM-*co*-AM)) copolymers, respectively. The synthesis and characterization of these polymers is reported elsewhere, along with a brief account of the viscosity in dilute solution.[45] The chemical structure of the hydrophobe groups is different from that in previous studies of HM−PAM associative polymers in which the hydrophobe was di-*n*-hexylacrylamide (DHAM).[25,26,46]

In this work, new insights are provided into the rheological and structural characteristics of hydrophobically modified polyacrylamide polymer gels. Shear rheometry experiments were performed to characterize the viscoelastic response of P(DPAM-*co*-AM) and P(DOAM-*co*-AM) gels as a function of the hydrophobe type, its content in the polymer, the length of the hydrophobe block, and temperature. The rheological behavior is expected to be characterized by multiple relaxation times, associated with the presence of multiple sticker sites per chain, in contrast to the rheology of telechelic polymers. Rheology provides information on the dynamics of the polymer network and on the strength of associations. This information is complemented with quantitative data from small-angle X-ray scattering (SAXS) experiments to probe network structure, in particular the correlation length and size of hydrophobic clusters.

2. Experimental Section

2.1. Materials. Hydrophobically modified polyacrylamide polymers, with disubstituted acrylamides DPAM and DOAM used as hydrophobic comonomers, are identical to those used before.[45] Copolymers with a blocky structure were synthesized using a micellar copolymerization route.[45]

Tables 1 and 2 show the weight-average molecular weight M_W for selected polymers determined via static light scattering (SLS).[45] Gel permeation chromatography (GPC) was undertaken for some samples. The results obtained by GPC were complicated by possible intermolecular association, even in the very dilute aqueous salt solutions employed. However, Table 2 shows M_W calculated by GPC for some copolymers for which SLS was not performed. The copolymer composition was determined by ^{1}H NMR spectroscopy in deuterium oxide (D_2O) according to literature methods.[46]

The polymer solutions were prepared by dissolution of polymers in Milli-Q filtered water at room temperature. The polymers were allowed to hydrate and swell for at least 24 hs; then the solutions were very gently stirred magnetically for 1 week to form homogeneous solutions. The polymer solutions were kept for another 5 days prior to measurement to remove air bubbles. All samples studied by rheology and SAXS were 4 wt % copolymer in water, which lies well above the overlap concentrations for these samples (below 0.1 wt %).[45]

The samples are denoted according to the nature of the hydrophobic comonomer. The sample code refers to the amount of hydrophobe, *f*, and the number of hydrophobic monomers per micelle, N_H, which is assumed to define the block length. For example, for sample 5DOAM4, the initial number indicates the hydrophobe concentration in the monomer feed $f = 5$ wt % and the final number indicates the value $N_H = 4$.

It is useful to estimate at this stage some parameters defining the mass and dimensions of the copolymers studied in this work. The molecular weight can be written as

$$M_w = nN_H M_H + n_P M_P \quad (1)$$

where n is the number of stickers per polymer chain (each sticker comprising N_H monomers), M_H is the molecular weight

Table 1. Characteristics of the P(DPAM-*co*-AM) Copolymers and Solutions

sample	M_w (g/mol) × 10^{-6}	R_G (Å)	n	l (Å)	R_l (Å)	τ_L (s)	G_o (Pa)	ξ (Å)	ΔR (Å)
1DPAM0.6	1.25[a]	241	133	251.3	14.7	0.03 (25 °C)	53.4 (25 °C)	36.2 (20 °C)	
						0.03 (30 °C)	43.4 (30 °C)	35.2 (30 °C)	
						0.03 (40 °C)	49 (40 °C)	33.8 (40 °C)	
						0.03 (56 °C)	17 (56 °C)	33.4 (50 °C)	
1DPAM1.3	1.62[a]	274.4	80	544.4	21.7			36.4 (20 °C)	
								35.1 (30 °C)	
								34.1 (40 °C)	
								32.8 (50 °C)	
1DPAM3.8	1.32[a]	247.7	22.2	1591.3	37.1	0.03 (25 °C)	29.4 (25 °C)	31.4 (20 °C)	
						0.03 (30 °C)	30.5 (30 °C)	31.9 (30 °C)	
						0.03 (40 °C)	28.9 (40 °C)	31.5 (40 °C)	
						0.04 (50 °C)	20.5 (50 °C)	31.1 (50 °C)	
1DPAM12	0.97[a]	212.3	5	5025.3	65.8	0.09 (25 °C)	12 (25 °C)		
3DPAM1.1	0.96[a]	209.9	163.9	153.5	11.5	0.13 (25 °C)	11.7 (25 °C)	39.9 (20 °C)	100.4 (20 °C)
						0.11 (30 °C)	14 (30 °C)	37.8 (30 °C)	64.0 (30 °C)
						0.11 (40 °C)	19 (40 °C)	37.3 (40 °C)	
						0.11 (50 °C)	9.8 (50 °C)	38.0 (50 °C)	
3DPAM1.5	0.87[a]	199.9	108.9	209.4	13.4	0.1 (25 °C)	2.8 (25 °C)	32.3 (20 °C)	
						0.09 (30 °C)	2.8 (30 °C)		
						0.09 (4 °C)	2.7 (40 °C)		
5DPAM1.1	1.16[a]	224.9	323.9	92.1	8.9	0.11 (25 °C)	14.5 (25 °C)	31.9 (20 °C)	
						0.09 (30 °C)	16.0 (30 °C)	30.7 (30 °C)	
						0.1 (40 °C)	3.2 (40 °C)	31.0 (40 °C)	
						0.1 (50 °C)	3.0 (50 °C)	30.5 (50 °C)	
5DPAM1.4	0.84[a]	195.2	184.3	117.2	10.1	0.11 (25 °C)	14.8 (25 °C)	34.2 (20 °C)	
						0.1 (30 °C)	13.6 (30 °C)	32.9 (30 °C)	
						0.1 (40 °C)	10.5 (40 °C)	32.8 (40 °C)	
						0.11 (50 °C)	11.8 (50 °C)	31.1 (50 °C)	
5DPAM4.0	1.2[a]	233.3	92.2	355.0	16.9	0.14 (25 °C)	16.8 (25 °C)	31.7 (20 °C)	30.7 (20 °C)
						0.3 (30 °C)	10.4 (30 °C)	30.6 (30 °C)	32.0 (30 °C)
						0.15 (40 °C)	7.5 (40 °C)	30.3 (40 °C)	32.6 (40 °C)
						0.09 (50 °C)	10.7 (50 °C)	30.4 (50 °C)	34.1 (50 °C)

[a] Data extracted from ref 45.

of a hydrophobic monomer, n_P is the number of polyacrylamide monomers and M_P is the molecular weight of one acrylamide monomer. Using the definition $f \approx (100nN_HM_H/n_PM_P)$ in eq 1, it is possible to estimate n_P:

$$n_P = \frac{M_w}{M_P(f/100 + 1)} \tag{2}$$

Values of n_P can be then calculated using M_W from Tables 1 and 2. The number of stickers per polymer chain can be then calculated from n_P and f, according to

$$n = \frac{fn_PM_P}{100N_HM_H} \tag{3}$$

The resulting n values are listed in Tables 1 and 2. Equation 3 can then be used to estimate the strand length between stickers

$$l = \frac{n_Pl_p}{n} \tag{4}$$

where l_p is the length of the carbon−carbon bond (1.54 Å). Values of l are listed in Tables 1 and 2. It is finally possible to crudely estimate the radius of gyration of the polymer chain as a whole assuming a random coil configuration

$$R_G = \frac{l_K}{\sqrt{6}}\sqrt{nN_H + n_P} \tag{5}$$

where l_K is the Kuhn length (estimated to be 4 Å). Similarly, the radius of gyration of the strand length is given by $R_l = l_K/(n_P/12n)^{1/2}$. Values obtained for R_G and R_l are listed in Tables 1 and 2. Values for R_G are expected to be an upper limit because intramolecular associations should lead to a contraction of the chain.

2.2. Rheological Measurements. Shear rheometry experiments were performed using a Rheometric Scientific SR5 controlled stress rheometer equipped with a cone-and- plate geometry (radius 2.0 cm, gap 0.038 mm) and a solvent trap that prevents evaporation of the samples during lengthy experiments. Measurements of the dynamic shear moduli were conducted for frequencies in the range $\omega = 0.1-100$ rad s^{-1} and temperatures $20 \le T \le 56$ °C. All measurements were carried out at frequencies and strains that led to a linear response. The polymer solution was gently loaded onto the plate and given about 30 min to allow the stresses to relax and to attain thermal equilibrium before starting measurements.

2.3. Small-Angle X-ray Scattering Experiments. SAXS measurements were performed using the setup at the University of Aarhus, which consists of a rotating anode, multilayer optics, three-pinhole collimation, an integrated vacuum system and a two-dimensional position-sensitive gas detector (HiSTAR).[47] The instrument is a modified version of the commercially available NanoSTAR equipment produced by Anton Paar, Graz, Austria, and distributed by Bruker AXS. The optimization of the instrument gives rise to a high flux and a low background, and it is therefore ideally suited for solution scattering. The samples were filled with a syringe into a quartz capillary, which is placed directly in the vacuum chamber of the camera. A home-built capillary holder with good thermal contact to the thermostated surrounding block was used, and measurements were conducted at temperatures between 20 and 50 °C. The instrument configuration gives access to a range of scattering vectors q between 0.01 and 0.35 $Å^{-1}$, where $q = (4\pi/\lambda)\sin\theta$, where 2θ is the scattering angle and λ is the wavelength. The two-dimensional spectra of all samples were isotropic and the data were azimuthally averaged, corrected for variations in detector efficiency, for spatial distortions and converted to an absolute scale using the scattering from pure water as a secondary standard.

Table 2. Characteristics of the P(DOAM-*co*-AM) Copolymers and Gels[a]

sample	M_w (g/mol) $\times 10^{-6}$	R_G (Å)	n	l (Å)	R_1 (Å)	τ_E, τ_C (s)	τ_R (s)	G_o (Pa)	ξ (Å)	ΔR (Å)
1DOAM0.2						67.8[d]	0.49 (20 °C)	183 (20 °C)[e]	19.9 (20 °C)	31.6 (20 °C)
						26.3 (30 °C)	0.07 (30 °C)	230 (30 °C)[e]	19.3 (30 °C)	31.5 (30 °C)
						10 (40 °C)	0.01 (40 °C)	333 (40 °C)[e]	17.3 (40 °C)	30.4 (40 °C)
						4.4 (50 °C)	0.002 (50 °C)	464 (50 °C)[e]	17.6 (50 °C)	28.6 (50 °C)
1DOAM0.3	0.617[b]	168.9	69	239.1	14.4	796.9[d]	0.21 (20 °C)	241 (20 °C)[e]		
							0.19 (30 °C)	224 (30 °C)[e]		
							0.25 (40 °C)	189 (40 °C)[e]		
						62.8 (50 °C)	0.1 (50 °C)	217 (50 °C)[e]		
1DOAM0.7	0.768[b]	188.4	37	557.9	21.9	195[d]	0.8 (20 °C)	185 (20 °C)[e]	34.3 (20 °C)	65.4 (20 °C)
							0.39 (30 °C)	193 (30 °C)[e]	35.6 (30 °C)	66.3 (30 °C)
						29.4 (40 °C)	0.2 (40 °C)	196 (40 °C)[e]	34.6 (40 °C)	65.4 (40 °C)
						11.3 (50 °C)	0.037 (50 °C)	268 (50 °C)[e]	34.6 (50 °C)	63.2 (50 °C)
1DOAM6.5								841.5 (20 °C)[f]		
								937.9 (30 °C)[f]		
								1072.7 (40 °C)[f]		
								1124.3 (50 °C)[f]		
3DOAM0.3	0.222[c]	100.5	73	79.7	8.3	176[d]	2.01 (20 °C)	248 (20 °C)[e]		
							0.53 (30 °C)	275 (30 °C)[e]		
						27.6 (40 °C)	0.43 (40 °C)	226 (40 °C)[e]		
						8.7 (50 °C)	0.08 (50 °C)	290 (50 °C)[e]		
3DOAM0.8	0.185[c]	91.8	23	212.5	13.5	8.3[d]	0.18 (20 °C)	111 (20 °C)[e]	21.2 (20 °C)	39.5 (20 °C)
						8.3 (20 °C)	0.09 (30 °C)	115 (30 °C)[e]	20.0 (30 °C)	38.4 (30 °C)
						3.3 (30 °C)	0.025 (40 °C)	150 (40 °C)[e]	19.6 (40 °C)	37.9 (40 °C)
						1.2 (40 °C)	0.002 (50 °C)	350 (50 °C)[e]	18.6 (50 °C)	37.1 (50 °C)
						0.5 (50 °C)				
3DOAM1.7							1.2 (40 °C)	478 (40 °C)[e]		
							0.38 (50 °C)	514 (50 °C)[e]		
5DOAM0.3						167.7[d]	0.17 (20 °C)	926 (20 °C)[e]	11.4 (20 °C)	30.7 (20 °C)
						44.9 (30 °C)	0.35 (30 °C)	627 (30 °C)[e]	11.9 (30 °C)	30.4 (30 °C)
						14.4 (40 °C)	0.12 (40 °C)	678 (40 °C)[e]	11.8 (40 °C)	30.0 (40 °C)
						5.6 (50 °C)	0.19 (50 °C)	416 (50 °C)[e]	11.8 (50 °C)	31.8 (50 °C)
5DOAM3.4									65.3 (20 °C)	47.7 (20 °C)
									61.2 (30 °C)	47.7 (30 °C)
									61.2 (40 °C)	48.9 (40 °C)
									65.3 (50 °C)	46.9 (50 °C)

[a] Polymer 5DOAM0.6 is omitted because relaxation time data could not be obtained for this sample. [b] Data extracted from ref 45. [c] Molecular weight determined by GPC. [d] Characteristic relaxation time taken from the crossover of G' and G'' in the time−temperature superposed curves ($T_0 = 20$ °C). [e] Data extracted from the fitting of the relaxation function. [f] Data extracted from the plateau of G' at high frequencies.

3. Results and Discussion

3.1. Rheology. In the following, the linear viscoelasticity of P(DPAM-*co*-AM) and P(DOAM-*co*-AM) samples is analyzed. The characteristic relaxation times of the samples are determined from the dynamic moduli G' and G''. At room temperature, P(DPAM-*co*-AM) samples were solutions, while the P(DOAM-*co*-AM) were gels.

The linear regime was located from stress sweep experiments. Confirmation of linear response was provided by the fact that G' and G'' were independent of the stress in stress sweep experiments for a set of imposed external frequencies in the range (0.1−100) rad s^{-1} (data not shown).

P(DPAM-*co*-AM) Copolymers. Frequency sweep experiments were performed in order to measure G' and G'' for solutions of 1DPAM0.6, 1DPAM3.8, 1DPAM12, 3DPAM1.1, 3DPAM1.5, 5DPAM1.1, 5DPAM1.4, and 5DPAM4.0 copolymers for temperatures in the range $25 \le T \le 56$ °C. Time−temperature superposition of the measured moduli was performed (reference temperature $T_0 = 25$ °C) to facilitate comparison of the frequency response at different temperatures. It was possible to superpose the storage and loss moduli for all the samples investigated, by shifting only the ω-coordinate by a temperature-dependent parameter a_T (Figure 1). The dependence of a_T with temperature could be satisfactorily fitted using the Williams−Landel−Ferry (WLF) equation[48] (Figure 1)

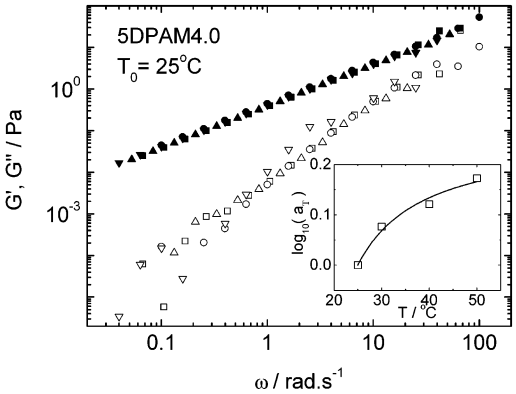

Figure 1. Frequency superposition for a 5DPAM4.0 solution. Storage modulus G' measured at (○) 25, (□) 30, (△) 40, and (▽) 50 °C and loss modulus G'' measured at (●) 25, (■) 30, (▲) 40, and (▼) 50 °C. The shear stress was fixed to $\sigma = 5$ Pa. The inset shows the temperature dependence of the frequency shift factor a_T: the full line is a fitting using the WLF equation.

$$\log a_T = -c_1(T - T_0)/(c_2 + T - T_0) \qquad (6)$$

with coefficients $c_1 = 0.26$ and $c_2 = 13.9$ °C.

Figure 1 suggests that there are no changes in the nature of the dynamic mechanical response as a func-

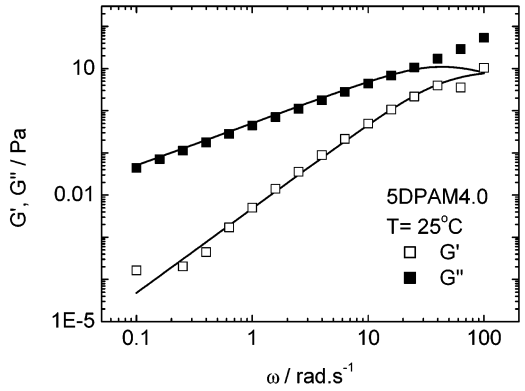

Figure 2. (□) Storage modulus G' and (■) loss modulus G'' as a function of frequency for a 5DPAM4.0 solution, measured at a shear stress $\sigma = 5$ Pa and temperature $T = 25$ °C. The full lines correspond to fits using the Maxwell model: $G'(\omega) = (G_0\omega^2\tau_L^2/1 + \omega^2\tau_L^2)$ and $G''(\omega) = (G_0\omega\tau_L/1 + \omega^2\tau_L^2)$.

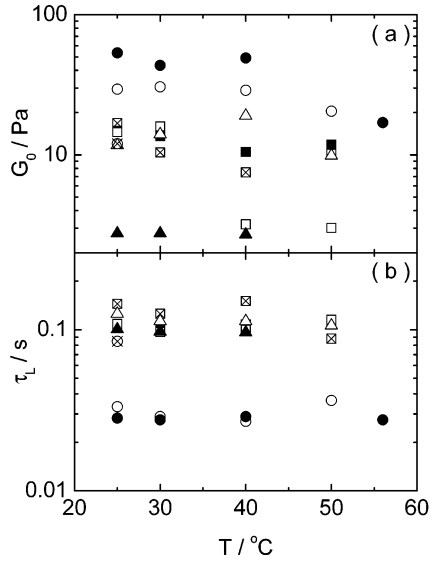

Figure 3. Temperature dependence of (a) the plateau modulus and (b) the relaxation time extracted from the fitting of G' and G'' using the Maxwell model for (●) 1DPAM0.6, (○) 1DPAM3.8, (⊗) 1DPAM12, (△) 3DPAM1.1, (▲) 3DPAM1.5, (□) 5DPAM1.1, (■) 5DPAM1.4 and (× in box) 5DPAM4.0 solutions.

tion of temperature. Similar to all other P(DPAM-*co*-AM) samples, the 5DPAM4.0 solution was in the liquid regime ($G'' > G'$) and the slopes of G' and G'' in the terminal zone were 1.8 and 1 respectively, independently of temperature, very close to the expected values (respectively 2 and 1) for a Maxwell fluid. Consistent with this, the low-frequency region was modeled using a Maxwell model, according to

$$G'(\omega) = \frac{G_0\omega^2{\tau_L}^2}{1 + \omega^2{\tau_L}^2} \qquad G''(\omega) = \frac{G_0\omega\tau_L}{1 + \omega^2{\tau_L}^2} \quad (7)$$

where the relaxation time τ_L and the plateau modulus G_0 were the fitting parameters.

Figure 2 shows a representative example of a fit to G' and G'' for a P(DPAM-*co*-AM) copolymer obtained using the Maxwell model. The parameters G_0 and τ_L obtained from fitting the full set of P(DPAM-*co*-AM) copolymer solutions studied are shown in parts a and b, respectively, of Figure 3 and Table 1. Comparing the experimental G' and G'' data and the Maxwell model calculations reveals important deviations at higher frequencies (Figure 2). The shape of the curves at higher frequencies is indicative of fast modes superimposed on a slow relaxation process. In fact, the current models describing the dynamics of associating polymers predict a multiple relaxation process (at least two characteristic times).[27] However, we will proceed at this stage to discuss the results obtained through the fitting of the low-frequency data.

It has been previously reported for acrylamide polymers modified with di-*n*-hexylacrylamide[25,26] that it was not possible to detect any trend in G_0 with the molecular weight or the hydrophobe characteristics, and that it remains constant for temperatures in the range $10 \leq T \leq 40$ °C.[25,26] In contrast, the results in Figure 3a show that, at approximately fixed M_W, for $f = 1$ and 3 wt % G_0 decreases upon increasing N_H, while there is a weak decrease of the plateau modulus with increasing temperature. For a fixed f, the strand length between stickers increases with increasing N_H (Table 1), leading to a lower sticker density and hence to a reduction of the plateau modulus. A decrease in G_0 upon increase of T can be ascribed to a decrease in the number of hydrophobic associations, reflecting an increase in solubility of the hydrophobic moieties, as already observed for acrylamide/ethylphenylacrylamide copolymers.[49]

The relaxation times obtained are similar to those previously reported for acrylamide polymers modified with di-*n*-hexylacrylamide.[25,26] For these polymers it was observed that the relaxation time of the system decreases upon increasing N_H[26] or the temperature.[25] The relaxation time τ_L can be ascribed to the lifetime of stickers associated in hydrophobic clusters. This relaxation time is found to be almost independent of temperature (Figure 3b and Table 1), in contrast to earlier reports on acrylamide polymers modified with di-*n*-hexylacrylamide, where the relaxation time was found to decrease with increasing temperature.[25] Regarding the dependence of the relaxation time on the hydrohobe content of the sample, τ_L is not sensitive to N_H but is sensitive to f since it is three times lower for $f = 1$ wt % than for $f = 3$ wt % and $f = 5$ wt %, reflecting the lower number of "stickers" for chains with $f = 1$ wt % (Figure 3b and Table 1). Only the relaxation time for 1DPAM12 is of the same order as those for the copolymers with $f = 3-5$ wt %, probably because the low f is balanced by a high N_H.

The theory of rubber elasticity was extended to transient networks by Green and Tobolsky. In their theory, the magnitude of the plateau modulus is related to ν, the number density of elastically active network strands per unit volume, through the expression[50]

$$G_0 = \nu k_B T \quad (8)$$

where k_B is the Boltzmann constant. It should be pointed out that the expression in eq 8 does not consider excluded volume interactions (probably present in our copolymer samples due to the existence of hydrophobic clusters), so this equation might not adequately describe the behavior of P(DPAM-*co*-AM) solutions, as has already been discussed for end-capped telechelic associative polymer solutions.[31] However, eq 8 will be used to estimate the fraction of active network strands per total number of chains, via [6,7,14] $\nu/n_C = G_0/n_C k_B T$, where $n_C = [\phi]N_A$ is the number density of chains in the solution, $[\phi]$ is the molar concentration of the solution, and N_A is Avogadro's number.

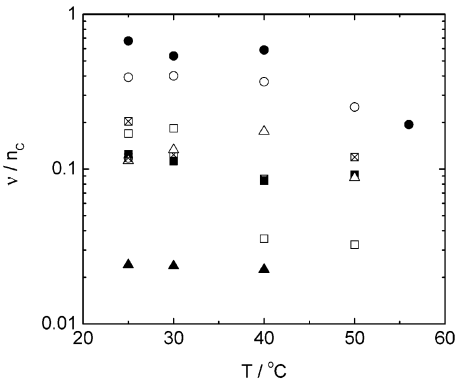

Figure 4. Temperature dependence of the fraction of active strands per total number of chains calculated using G_0 values shown in Figure 3a and Table 1 for (●) 1DPAM0.6, (○) 1DPAM3.8, (⊗) 1DPAM12, (△) 3DPAM1.1, (▲) 3DPAM1.5, (□) 5DPAM1.1, (■) 5DPAM1.4 and (× in box) 5DPAM4.0 solutions.

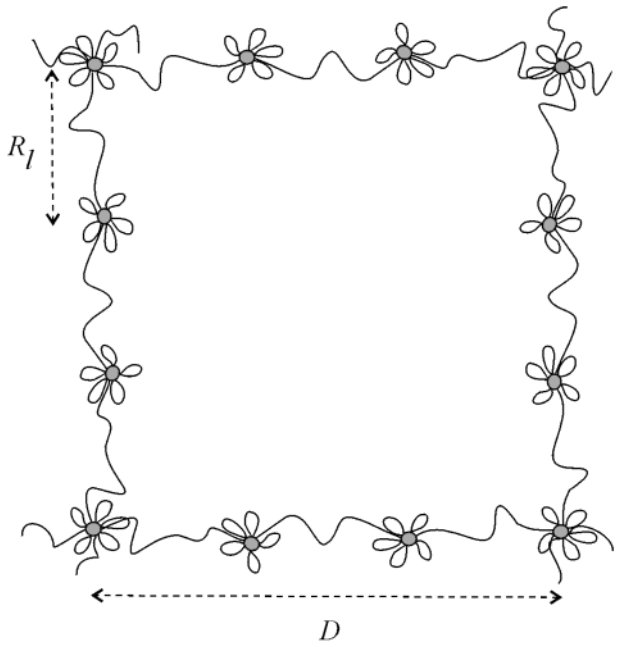

Figure 5. Schematic illustration of the definition of the radius of gyration of the strand length, R_l, and the average mesh size of the network, D, related to a state of chain association.

Figure 4 shows the temperature dependence of the fraction of active strands with respect to the total number of chains, calculated using values of G_0 shown in Figure 3a and Table 1. It is evident that the dependences of (ν/n_C) on f and T are similar to those for G_0, and therefore will not be discussed here. It is worth noting however that (ν/n_C) is always less than 1.

Hydrophobic clusters in a P(DPAM-*co*-AM) solution result from associations between stickers in the polymeric chains. Stickers in the same chain can be associated with different hydrophobic clusters. The average "mesh size" of the network (Figure 5) can be estimated as

$$D = (k_B T/G_0)^{1/3} \tag{9}$$

Using the data in Figure 3a, values of D correspond, on average over all the temperatures, to D = 493.2, 541.7, and 699.8 Å for 1DPAM0.6, 1DPAM3.8, and 1DPAM12 respectively, D = 688 and 1154.3 Å for 3DPAM1.1 and 3DPAM1.5 respectively and finally D = 885.5, 691.7, and 735.6 Å for 5DPAM1.1, 5DPAM1.4, and 5DPAM4.0. It should be observed that, since it is inversely proportional to G_o, D increases upon increasing N_H for f = 1 and 3 wt %, probably reflecting the increase of R_l with N_H (Table 1).

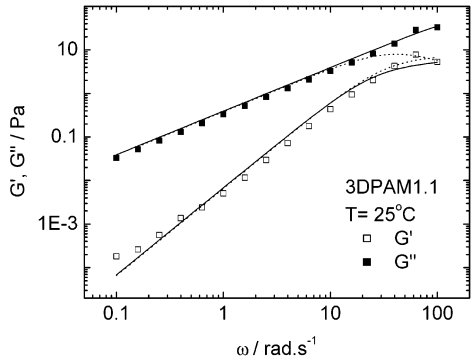

Figure 6. (□) Storage modulus G' and (■) loss modulus G'' as a function of frequency for a 3DPAM1.1 solution, measured at a shear stress σ = 5 Pa and temperature T = 25 °C. The full lines correspond to fits using two relaxation times (eq 10). The dotted lines correspond to fits using the Maxwell model (eq 7).

Returning to the modeling of the dynamic shear moduli, an improvement to the fitting of the dynamic data obtained through the Maxwell model calculations (eq 7, Figure 2) can be obtained using two relaxation times. We have fitted the frequency dependence of G' and G'' using two characteristic times, for a 3DPAM1.1 solution, according to

$$G'(\omega) = G_0 \sum_{i=1}^{2} \frac{\mu_i \omega^2 {\tau_i}^2}{1+\omega^2 {\tau_i}^2} \qquad G''(\omega) = G_0 \sum_{i=1}^{2} \frac{\mu_i \omega \tau_i}{1+\omega^2 {\tau_i}^2} \tag{10}$$

where μ_1 and μ_2 are the weights of the relaxation times τ_1 and τ_2 respectively (Figure 6). The corresponding fitting using a Maxwell model (considering only one relaxation time τ_L) is also shown in Figure 6. The fits to the two Maxwell elements model provided τ_1 = 0.13 s and τ_2 = 0.02 s. In agreement with the discussion above, $\tau_1 = \tau_L$ (Table 1, Figure 3b) dominates at low frequencies and can be identified as the slow mode of the system, while the additional fast mode τ_2 is superimposed on the slow mode process and improves the fitting of G' and G'' at high frequencies.

P(DOAM-*co*-AM) Copolymers. The increased hydrophobicity of DOAM compared to DPAM resulted in gels for these copolymers (despite the lower molecular weight of the former polymers). In particular, for some P(DOAM-*co*-AM) copolymer gels, it was observed that $G' > G''$ even at lower frequencies.

Frequency sweep experiments were performed for 1DOAM0.2, 1DOAM0.3, 1DOAM0.7, 1DOAM6.5, 3DOAM0.3, 3DOAM0.8, 3DOAM1.7, 5DOAM0.3, 5DOAM0.6, and 5DOAM3.4 gels for temperatures in the range 20 ≤ T ≤ 50 °C. Time−temperature superposition of the measured moduli (T_0 = 20 °C) enabled comparison of the frequency response at different temperatures. It was possible to superpose the storage and loss moduli for all the samples investigated, by shifting the moduli along the logarithmic frequency scale by a temperature-dependent parameter a_T and also, when necessary, by a weakly temperature-dependent vertical shift factor a_m. It was not possible to measure a crossover of G' and G'' for 1DOAM6.5, 3DOAM1.7, 5DOAM0.6, and 5DOAM3.4 gels, although it could be

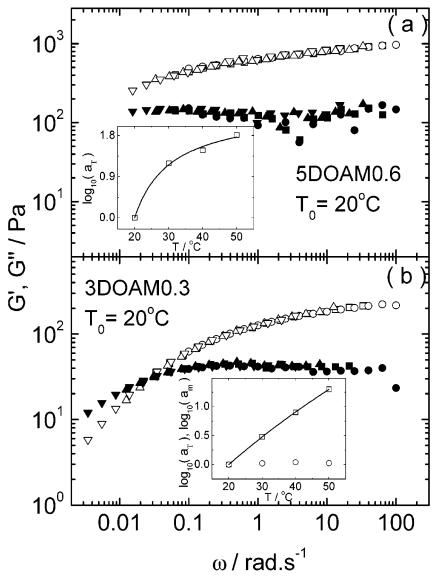

Figure 7. Frequency and moduli simultaneous superposition for gels of (a) 5DOAM0.6 and (b) 3DOAM0.3. Storage modulus G' measured at (○) 20, (□) 30, (△) 40, and (▽) 50 °C and loss modulus G'' measured at (●) 20, (■) 30, (▲) 40, and (▼) 50 °C. The shear stress was fixed to $\sigma = 1$ Pa. The inset shows the temperature dependence of the frequency shift factor (□) a_T and the moduli shift factor (○) a_m: the full line is a fit using the WLF equation.

clearly observed for the others. Figure 7 contains representative superposed frequency sweeps for 5DOAM0.6 and 3DOAM0.3. A crossover of G' and G'' is observed for the latter, but not the former. The larger N_H and f in 5DOAM0.6 produces a noticeably more elastic gel than that formed by 3DOAM0.3. The insets in Figure 7 show the temperature dependence of the shift factors. Similar to Figure 1, the insets in Figure 7 show that the dependence of a_T with the temperature could be satisfactorily fitted using the WLF equation,[48] with c_1 = 2.4 and 9.4 and c_2 = 10.7 °C and 187.1 °C for 5DOAM0.6 and 3DOAM0.3, respectively. Finally, the shallow and wide minimum in G'' for 5DOAM0.6 indicates a very broad distribution of relaxation times in the system.

The success of the time−temperature superposition (Figure 7), shows that, similarly to the P(DPAM-*co*-AM) solutions, the nature of the dynamic mechanical response of the P(DOAM-*co*-AM) gels does not change as a function of temperature. Table 2 shows the characteristic relaxation time, τ_C, taken from the crossover of G' and G'' in the time−temperature superposed curves (T_0 = 20 °C).

The characteristic time, τ_E, measured from the crossover of G' and G'' in the original (nonsuperposed) experimental data at higher temperature is also shown in Table 2. The results in Table 2 show that $\tau_E \leq \tau_C$, as expected since $a_T \geq 1$. No trend for the dependence of τ_E on N_H can be discerned. However, τ_E decreases upon increasing f, for fDOAM0.3 samples (Table 2). The higher molecular weight of 1DOAM0.3 in relation to 3DOAM0.3 (Table 2), suggests that the apparent counterintuitive decrease of τ_E with f is actually due to the fact that τ_E depends more strongly on M_W than on f, as predicted by the sticky reptation model.[27]

Additional information about the P(DOAM-*co*-AM) gel structure can be obtained from the value of G' (at a particular frequency) as a function of f. Figure 8 shows G' for 1DOAM0.3, 3DOAM0.3, and 5DOAM0.3, at 20 °C. There is clearly an increase in G', at any frequency, with increasing f, probably because upon increasing f at fixed N_H, the length between stickers decreases enhancing hydrophobic cluster associations, leading to a stiffer gel (Table 2).

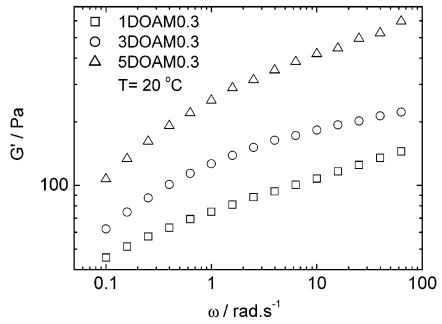

Figure 8. Frequency dependence of the storage modulus G' for gels of (□) 1DOAM0.3, (○) 3DOAM0.3, and (△) 5DOAM0.3 at 20 °C.

The frequency dependence of the dynamic shear moduli for the P(DOAM-*co*-AM) samples indicates a broad distribution of relaxation times. This complicates the analysis. Fitting using multiple Maxwell elements was possible. However, a simpler and more model-independent approach was adopted, by calculating the relaxation modulus $G(t)$. This function was computed for selected P(DOAM-*co*-AM) samples. The dynamic modulus was converted to stress relaxation data through a Fourier transformation, using the Orchestrator program provided by Rheometric Scientific Inc.

The time-dependent stress relaxation function determines an elastic plateau modulus G_0 and a characteristic relaxation time, τ_R, through fitting to a stretched exponential,

$$G(t) = G_0 \exp[-(t/\tau_R)^{\alpha}] \qquad (11)$$

where α is an exponent which is allowed to vary.

A stretched exponential describes the form of $G(t)$ very well, as exemplified by Figure 9a which shows representative fits to $G(t)$ for the 1DOAM0.2 gel. The frequency range of the dynamic data used to calculate $G(t)$ is shown in Figure 9b. The dependence of τ_R on temperature for the full set of $G(t)$ modeled through eq 11 is shown in Figure 10 and Table 2. Values of α were in the range 0.2−0.4, independent of temperature and polymer composition. Somewhat larger values have been reported for telechelic F−HEUR polymers (α = 0.7−0.9). A stretched exponential decay is typical for complex, slowly relaxing, strongly interacting materials.[14]

The plateau modulus G_o slightly increases upon increasing temperature in the range 10 ≤ T ≤ 50 °C for the P(DOAM-*co*-AM) samples (with the exception of 5DOAM0.3), suggesting that the entropic network elasticity outweighs any change in hydrophobe association number. Considering the dependence on hydrophobe content for the fDOAM0.3 series, it is found that G_0 increases upon increasing f at a fixed temperature in agreement with the trend of G' as a function of f discussed earlier (Figure 8).

It is useful at this stage to compare τ_R with τ_E (Table 2 and Figure 10). The immediate observation is that τ_E is on average 3 orders of magnitude higher than τ_R, as expected since τ_R is obtained from the high-frequency modulus data. We will then identify τ_R and τ_E as the fast and slow relaxation times of the system, respec-

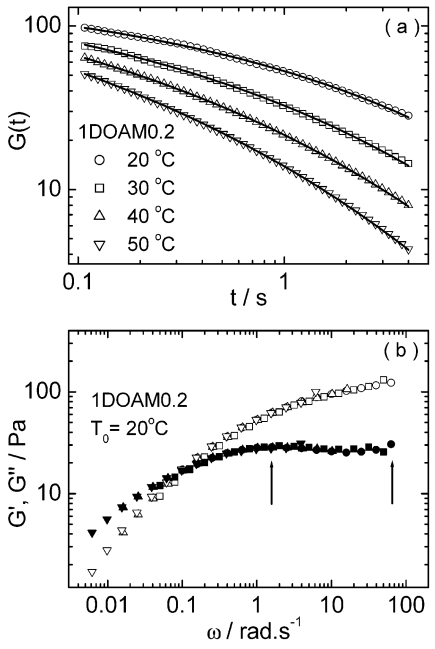

Figure 9. (a) Time dependence of the stress relaxation function $G(t)$ for 1DOAM0.2 gel at (○) 20, (□) 30, (△) 40, and (▽) 50 °C. The full lines correspond to a fitting using a stretched exponential. (b) Time−temperature superposition for the 1DOAM0.2 gel: storage modulus G' measured at (○) 20, (□) 30, (△) 40, and (▽) 50 °C and loss modulus G'' measured at (●) 20, (■) 30, (▲) 40, and (▼) 50 °C. The shear stress was fixed to $\sigma = 1$ Pa. The arrows show the range of frequencies used for the calculation of $G(t)$.

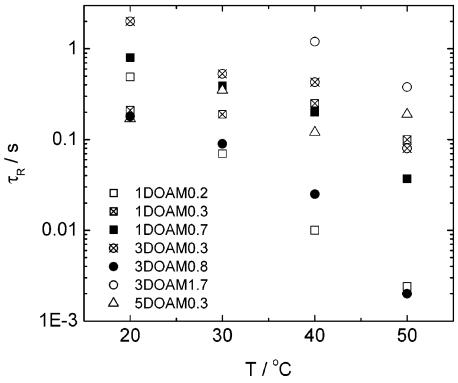

Figure 10. Temperature dependence of the relaxation time τ_R extracted from the fitting of $G(t)$ using a stretched exponential for gels of (□) 1DOAM0.2, (× in a box) 1DOAM0.3, (■) 1DOAM0.7, (⊗) 3DOAM0.3, (●) 3DOAM0.8, (○) 3DOAM1.7, and (⊗) 5DOAM0.3.

tively. The set of relaxation times in Figure 10 do not show any particular trend with N_H or f, although a decrease of τ_R with increasing T can be clearly observed.

Solutions of acrylamide polymers modified with di-*n*-hexylacrylamide, have been characterized with one relaxation time,[25,26] which decreased with increasing temperature. The relaxation time was initially obtained from the crossover of G' and G''.[25] However, because this occurred at high frequency, the value obtained is comparable to our τ_R. Subsequently a relaxation time was obtained in the low-frequency limit that is comparable to our τ_E.[26]

Finally, although the determination of the parameter (ν/n_C) was only restricted to a few samples, due to the molecular weight data available (Table 2), it was calculated for 1DOAM0.3, 1DOAM0.7, 3DOAM0.3, and 3DOAM0.8 gels, using the values of G_0 in Table 2. Briefly, the calculation provided on average over all the temperatures $(\nu/n_C) = 1.3$, 1.6, 0.6, and 0.3 for 1DOAM0.3, 1DOAM0.7, 3DOAM0.3, and 3DOAM0.8 gels, respectively. It should be mentioned that, in contrast to telechelics where (ν/n_C) is always lower than one, this parameter can be higher than one for P(DOAM-*co*-AM) gels due to the particularly large number of stickers per chain (Table 2).

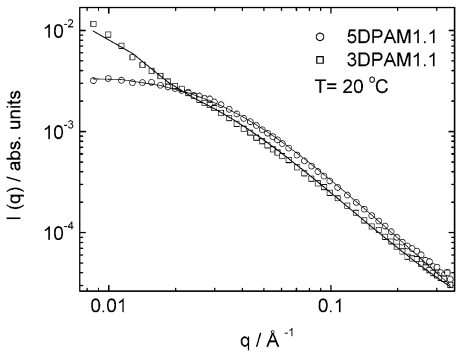

Figure 11. Small-angle X-ray scattering curves for (□) 3DPAM1.1 and (○) 5DPAM1.1 solutions at 20 °C. The full lines correspond to the fitting using an asymptotic Lorentzian dependence for the scattered intensity. Local fluctuations in the concentration were considered for 3DPAM 1.1 solution.

3.2. Small-Angle X-ray Scattering. SAXS experiments were performed in an attempt to determine the correlation length and the size of the hydrophobic clusters in the P(DPAM-*co*-AM) solutions and P(DOAM-*co*-AM) gels.

P(DPAM-*co*-AM) Copolymers. The mesoscopic structure of solutions of 1DPAM0.6, 1DPAM1.3, 1DPAM3.8, 3DPAM1.1, 3DPAM1.5, 5DPAM1.1, 5DPAM1.4, and 5DPAM4.0 was probed by SAXS for temperatures in the range $20 \leq T \leq 50$ °C.

The shape of the SAXS curves changed very little with temperature. Since the general features of the SAXS curves were similar for the full set of copolymer solutions, only the two curves presenting extreme differences are shown in Figure 11 for solutions of 3DPAM1.1 and 5DPAM 1.1 at 20 °C.

For a polymer solution in a good solvent the polymer−polymer correlation function is given for distances $r \geq \xi$, where ξ is the correlation length of the polymer density fluctuations in the solution, by the function[51]

$$\epsilon(r) = \frac{\xi}{r}\exp\left(-\frac{r}{\xi}\right) \tag{12}$$

The corresponding scattering function is Lorentzian:[52]

$$I(q) \propto \left(\frac{2}{\pi}\right)^{1/2}\frac{\langle c\rangle^2\xi^2}{(1+q^2\xi^2)} \tag{13}$$

where $\langle c\rangle$ is the average polymer concentration.

SAXS curves for solutions of 1DPAM0.6, 1DPAM1.3, 1DPAM3.8, 3DPAM1.5, 5DPAM1.1, and 5DPAM1.4 could be modeled according to eq 13. However, in order to model the SAXS curves for some samples with high hydrophobe content, i.e., solutions of 3DPAM1.1 and 5DPAM4.0, it was necessary to add an additional term to eq 13, which allows for spatial heterogeneities due to the enhanced hydrophobe density in the vicinity of hydrophobic clusters. If the clusters are localized and

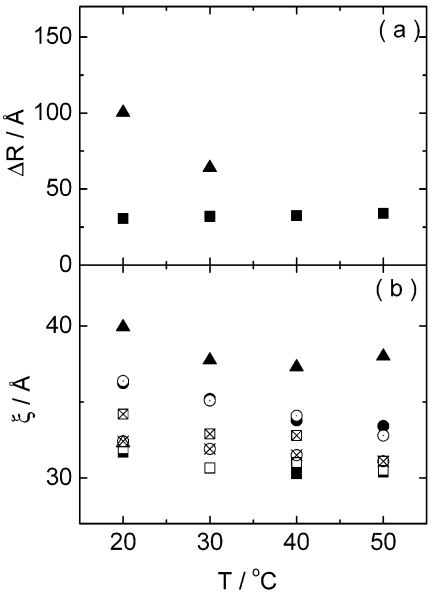

Figure 12. Temperature dependence of (a) characteristic size of concentration fluctuations and (b) correlation length for solutions of (●) 1DPAM0.6, (⊙) 1DPAM1.3, (⊗) 1DPAM3.8, (▲) 3DPAM1.1, (△) 3DPAM1.5, (□) 5DPAM1.1, (× in box) 5DPAM1.4, and (■) 5DPAM4.0.

positioned randomly, they can be described by a Gaussian with a characteristic length ΔR, and we obtain[52]

$$I(q) \propto \left(\frac{2}{\pi}\right)^{1/2} \frac{\langle c\rangle^2 \xi^2}{(1+q^2\xi^2)} + \langle \Delta c^2\rangle \, \Delta R^2 \exp\left(-\frac{\Delta R^2 q^2}{2}\right) \quad (14)$$

It is implicitly assumed in eq 14 that polymer concentration fluctuations are decoupled from hydrophobe density fluctuations,[53] i.e., the two order parameters are independent.

Figure 11 shows fits to the SAXS curves obtained for 5DPAM1.1 and 3DPAM1.1 solutions using eqs 13 and 14, respectively. The full set of ΔR and ξ parameters extracted from the fitting to the SAXS curves through eqs 13 and 14, are shown in Figure 12 and Table 1. The correlation length ξ decreases with increasing temperature. This trend is expected as solvent quality improves with increasing temperature and also thermal fluctuations increase with temperature.

P(DOAM-*co*-AM) Copolymers. The structure of gels of 1DOAM0.2, 1DOAM0.7, 3DOAM0.8, 5DOAM0.3, and 5DOAM3.4 was probed by SAXS for temperatures in the range $20 \le T \le 50$ °C. Similarly to the P(DPAM-*co*-AM) copolymer gels, the SAXS curves were not extremely sensitive to the copolymer composition. Figure 13 shows SAXS curves for 1DOAM0.2, 1DOAM0.7, 3DOAM0.8, and 5DOAM0.3 gels at 20 °C, fitted to eq 14 (the fitting to eq 13 is not satisfactory, as shown in Figure 13c). The parameters extracted from the modeling are plotted in Figure 14 and shown in Table 2 as a function of temperature.

The results in Figure 14 and Table 2 show that both the hydrophobe density fluctuations (characteristic size ΔR) and the correlation length increase strongly with N_H. This result differs from that for P(DPAM-*co*-AM) copolymer solutions. It is possible that for P(DOAM-*co*-AM) copolymer gels, the growth in size of the hydrophobic aggregates (with N_H) increases the volume fraction of aggregates in the system and favors a local order condition in which the correlation length is also

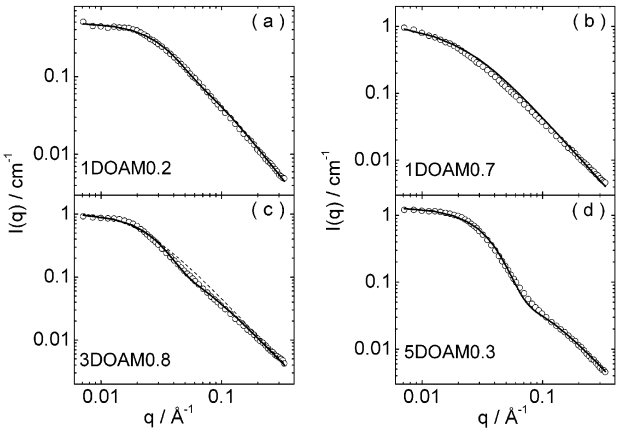

Figure 13. (○) Small-angle X-ray scattering curves for (a) 1DOAM0.2, (b) 1DOAM0.7, (c) 3DOAM0.8, and (d) 5DOAM0.3 gels at 20 °C. The full lines correspond to the fitting using an asymptotic Lorentzian dependence for the scattered intensity, considering local fluctuations in the concentration. The dashed lines corresponds to the fitting obtained using only a Lorentzian function.

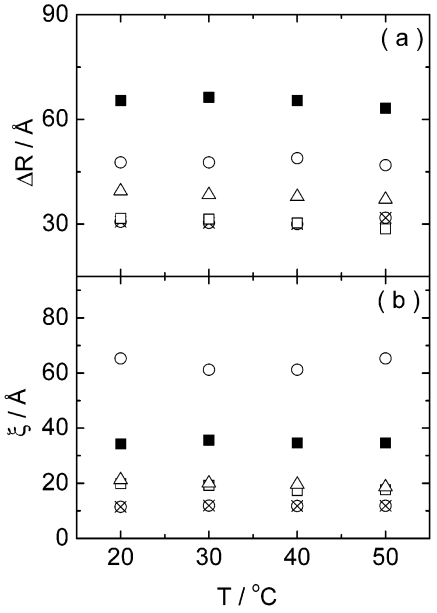

Figure 14. Temperature dependence of (a) characteristic size of concentration fluctuations and (b) correlation length for gels of (□) 1DOAM0.2, (■) 1DOAM0.7, (△) 3DOAM0.78, (⊗) 5DOAM0.3 and (○) 5DOAM3.4.

increased. It is also apparent that for the P(DOAM-*co*-AM) samples, in contrast to the P(DPAM-*co*-AM) solutions, ΔR and ξ are almost independent of temperature—this is consistent with stronger associations between hydrophobes.

4. Conclusions

This work provides new insights into the rheological and structural properties of a series of hydrophobically modified polyacrylamides. Two series of polyacrylamide-based copolymers containing hydrophobic DPAM and DOAM comonomers have been characterized using rheology and SAXS.

Because of the high hydrophobicity of DOAM comonomers, P(DOAM-*co*-AM) copolymers formed gels characterized by multiple relaxation modes analyzed through $G(t)$. In contrast, P(DPAM-*co*-AM) copolymers formed solutions which were characterized by a response de-

scribed essentially by a single Maxwell element although an additional fast mode was evident at high frequencies. The plateau modulus G_0 for P(DOAM-*co*-AM) copolymer gels is an order of magnitude higher than for P(DPAM-*co*-AM) copolymer solutions (Tables 1 and 2) despite the lower molecular weight.

Rheology allowed the determination of the lifetime of associations between stickers in the hydrophobic clusters for P(DPAM-*co*-AM) and P(DOAM-*co*-AM) copolymers. A decrease in the number of hydrophobic associations upon increasing temperature was observed for P(DPAM-*co*-AM) copolymers suggesting that sticker dissociation is favored. In contrast, for P(DOAM-*co*-AM) copolymers, the entropic network elasticity outweighs any change in hydrophobe association number upon increasing temperature.

The P(DPAM-*co*-AM) solution structure measured by SAXS was typical of polymer solutions in good solvent conditions. Additional heterogeneous concentration fluctuations had to be considered for the P(DOAM-*co*-AM) polymers with higher hydrophobe content.

References and Notes

(1) Glass, J. E., Ed. *Water-soluble polymers: Beauty with Performance*; American Chemical Society: Washington, DC, 1986; Vol. 213.
(2) Glass, J. E., Ed. *Hydrophilic Polymers: Performance with Environmental Acceptability*; American Chemical Society: Washington, DC, 1996; Vol. 248.
(3) Shalaby, S. W., McCormick, C. L., Butler, G. B., Eds. *Water-soluble polymers. Synthesis, Solution Properties and Applications*; American Chemical Society: Washington, DC, 1991; Vol. 467.
(4) Winnik, M. A.; Yekta, A. *Curr. Opin. Colloid Interface Sci.* **1997**, *2*, 424.
(5) Schulz, D. N., Glass, J. E., Eds. *Polymers as Rheology Modifiers*; ACS Symposium Series 462; American Chemical Society: Washington, DC, 1991.
(6) Annable, T.; Buscall, R.; Ettelaie, R. *Colloids Surf. A* **1996**, *112*, 97.
(7) Annable, T.; Buscall, R.; Ettelaie, R.; Whittlestone, D. *J. Rheol.* **1993**, *37*, 695.
(8) Jenkins, R. D. Ph.D. Thesis. Lehigh University: Bethlehem, PA, 1990.
(9) Jenkins, R. D.; Silebi, C. A.; El-Aasser, M. S. *Polym. Mater. Eng. Sci.* **1989**, *61*, 629.
(10) Hwang, F. S.; Hogen-Esch, T. E. *Macromolecules* **1993**, *26*, 3156.
(11) Hwang, F. S.; Hogen-Esch, T. E. *Macromolecules* **1995**, *28*, 3328.
(12) Xie, X.; Hogen-Esch, T. E. *Macromolecules* **1996**, *29*, 1734.
(13) Zhang, Y.-X.; Da, A.-H.; Butler, G. B.; Hogen-Esch, T. E. *J. Polym. Sci.* **1992**, *30*, 1383.
(14) Calvet, D.; Collet, A.; Viguier, M.; Berret, J. F.; Séréro, Y. *Macromolecules* **2003**, *36*, 449.
(15) Zhang, H.; Hogen-Esch, T. E.; Boschet, F.; Margaillian, A. *Polym. Prepr. (Am. Chem. So., Div. Polym. Chem.)* **1996**, *37*, 731.
(16) Cathébras, N.; Collet, A.; Viguier, M. *Macromolecules* **1998**, *31*, 1305.
(17) Tae, G.; Kornfield, J. A.; Hubbell, J. A.; Lal, J. *Macromolecules* **2002**, *35*, 4448.
(18) English, R. J.; Gulati, H. S.; Jenkins, R. D.; Khan, S. A. *J. Rheol.* **1997**, *41*, 427.
(19) English, R. J.; Raghavan, S. R.; Jenkins, R. D.; Khan, S. A. *J. Rheol.* **1999**, *43*, 1175.
(20) Evani, S. US Patent 4 432 881, 1982.
(21) Turner, S. R.; Siano, D. B.; Bock, J. US Patent 4 520 182, 1985.
(22) Candau, F.; Heatley, F.; Price, C.; Stubbersfield, R. B. *Eur. Polym. J.* **1984**, *20*, 685.
(23) Xue, W.; Hamley, I. W. *Polymer* **2002**, *43*, 3069.
(24) Xue, W.; Hamley, I. W.; Huglin, M. B. *Polymer* **2002**, *43*, 5181.
(25) Volpert, E.; Selb, J.; Candau, F. *Polymer* **1998**, *39*, 1025.
(26) Jiménez Regalado, E.; Selb, J.; Candau, F. *Macromolecules* **1999**, *32*, 8580.
(27) Leibler, L.; Rubinstein, M.; Colby, R. H. *Macromolecules* **1991**, *24*, 4701.
(28) Palmer, R. G.; Stein, D. L.; Abrahams, E.; Anderson, P. W. *Phys. Rev. Lett.* **1984**, *53*, 958.
(29) Annable, T.; Buscall, R.; Ettelaie, R. In *Amphiphilic Block Copolymers: Self-assembly and Applications*; Lindman, B., Ed.; Elsevier: Amsterdam, 2000; p 281.
(30) Ng, W. K.; Tam, K. C.; Jenkins, R. D. *J. Rheol.* **2000**, *44*, 137.
(31) Pham, Q. T.; Russel, W. B.; Thibault, J. C.; Lau, W. *Macromolecules* **1999**, *32*, 5139.
(32) Séréro, Y.; Jacobsen, V.; Berret, J. F.; May, R. *Macromolecules* **2000**, *33*, 1841.
(33) Hecht, A. M.; Duplessix, R.; Geissler, E. *Macromolecules* **1985**, *18*, 2167.
(34) Shibayama, M.; Tanaka, T.; Han, C. C. *J. Chem. Phys.* **1992**, *97*, 6829.
(35) Witten, T. A. *J. Phys. (Paris)* **1988**, *49*, 1055.
(36) Semenov, A. N.; Joanny, J. F.; Khokhlov, A. R. *Macromolecules* **1995**, *28*, 1066.
(37) Semenov, A. N.; Nyrkova, I. A.; Khokhlov, A. R. *Macromolecules* **1995**, *28*, 7491.
(38) Nyrkova, I. A.; Khokhlov, A. R.; Doi, M. *Macromolecules* **1993**, *26*, 3601.
(39) Rubinstein, M.; Semenov, A. N. *Macromolecules* **1998**, *31*, 1386.
(40) Borisov, O. V.; Halperin, A. *Macromolecules* **1995**, *11*, 2911.
(41) Borisov, O. V.; Halperin, A. *Macromolecules* **1996**, *29*, 2612.
(42) Khalatur, P. G.; Khokhlov, A. R.; Nyrkova, I. A.; Semenov, A. N. *Macromol. Theory Simul.* **1996**, *5*, 713.
(43) de Groot, R.; Agterof, W. G. M. *Macromolecules* **1995**, *28*, 6284.
(44) Kumar, S. K.; Panagiotopoulos, A. Z. *Phys. Rev. Lett.* **1999**, *82*, 5061.
(45) Xue, W.; Hamley, I. W.; Castelletto, V.; Olmsted, P. *Eur. Polym. J.* **2004**, *40*, 47.
(46) Volpert, E.; Selb, J.; Candau, F. *Macromolecules* **1996**, *29*, 1452.
(47) Pedersen, J. S. *J. Appl. Crystallogr.* **2003**, to be submitted.
(48) Ferry, J. D. *Viscoelastic Properties of Polymers*; Wiley: London, 1980.
(49) Biggs, S.; Selb, J.; Candau, F. *Polymer* **1993**, *34*, 580.
(50) Green, M. S.; Tobolsky, A. V. *J. Chem. Phys.* **1946**, *14*, 80.
(51) de Gennes, P. G. *Scaling Concepts in Polymer Physics*; Cornell University Press: Ithaca, NY, 1979.
(52) Mallam, S.; Hecht, A. M.; Geissler, E.; Pruvost, P. *J. Chem. Phys.* **1989**, *91*, 6447.
(53) Mallam, S.; Horkay, F.; Hecht, A.-M.; Rennie, A. R.; Geissler, E. *Macromolecules* **1991**, *24*, 543.

MA035039D